Electronic Supplementary Material (ESI) for Molecular BioSystems

Supplementary Material

Mass Spectrometry–based Identification and Characterisation of Lysine and Arginine Methylation in the Human Proteome

M. Bremang[a,†], A. Cuomo[a,†], A. M. Agresta[a,‡], M. Stugiewicz[a], V. Spadotto[a] and T. Bonaldi[a,*]

Supplementary Experimental

Estimation of incorporation efficiency

Incorporation of L-[$^{13}CD_3$]-Methionine (Met-4, heavy) was tested for HeLaS3 cells cultivated in "heavy" medium after 9 replication cycles. Whole cell extracts from HeLaS3 heavy-labeled were subjected to GeLCMS analysis (see Experimental Section in the main text). Raw data from LTQ-Orbitrap Velos were than processed by MaxQuant software 1.3.0.5, as described in the Experimental section, disabling the re-quantify option[1]. Incorporation percentage was calculated by applying to non-redundant peptide ratios, automatically extracted by a customized R script, using the following formula: *Incorporation rate (%) = ratio (H/L)/ ratio (H/L) +1 ×100*.

Western blot analysis

The two different whole-cell protein extracts (prepared in Urea or Ripa buffer) were separated by SDS-PAGE electrophoresis, blotted on the PVDF membrane and incubated with tested antibodies. The following antibodies were used according to the manufacturer's instructions: AR-K_{pan} (Acris APO 9328PU-N, dilution 1:1000), LS-K_{pan} (LifeSpan Biosciences LS-C60093/28979, dilution 1:1000), AC-$K_{me,di}$ (AbCam Ab23366 dilution 1:500), IC-$K_{me,di/tr}$ (Immunechem ICP0501/ICP0601, dilution 1:2000), AC-K_{tr} (AbCam Ab76118, dilution 1:1000), CS-R_{me-I} (Cell Signaling Technology D5A12, dilution 1:1000), CS-R_{me-II} (Cell Signaling Technology Me-R4-100, dilution 1:1000), EG-R_{sym} (E. Guccione (IMCB) Rabbit 2 (SYM), dilution 1:1000) MP-R_{sym} (Merck Millipore SYM10, dilution 1:1000) EG-R_{asym} (E. Guccione (IMCB) Rabbit 1 (ASYM), dilution 1:1000), MP-R_{asym} (Merck Millipore ASYM24, dilution 1:1000). Vinculin was used as the loading control as well as Ponceau-stained core histones, blotted on the PVDF membrane.

Supplementary Figure and Table Legends

Figure S1. Monitoring cell growth in hmSILAC media and incorporation analysis. (A) Growth curves of HeLaS3 cells, cultured in normal (blue) or hmSILAC media (red). No differences in doubling time observed between the two cell populations. **(B)** Full-MS spectrum of the methionine-containing peptide LQIVEMPLAHK shows a H/L ratio of 9:1, reflecting the measured rate of incorporation (green: heavy; black: light). The extracted ion chromatogram (XIC) for both Heavy and Light forms of the same peptide is also reported on the right panel (green: heavy; black: light). **(C)** Unimodal distribution of H/L ratios for tryptic peptides from extracts of HeLaS3 grown in Met-4 SILAC medium after 9 doublings. The mode of the distribution is 0.97 and describes the vast majority of peptides, indicating an incorporation rate of 97% for methionine-containing peptides.

Figure S2. Detection of methylated proteins by anti-methyl-K/R antibodies. Left panels: Examples of anti-methyl antibody specificity testing: HeLaS3 cells treated with increased amounts of the methyltransferase inhibitor AdOx, for 24 and 48 hours were resolved on SDS-PAGE and probed with different pan-methyl antibodies. Right panels: Western blots with the same antibodies after a wash-out (WO) experiment, where cells were treated with 40 µM AdOx for 72h, then the inhibitor was washed out and cells allowed to grow for another 72hrs, then harvested and the extract probed with anti-methyl antibodies.

Figure S3. Comparison of anti-pan-methyl-K antibody performance and In-Gel Intensity distribution. (**A**) Venn Diagram describing the contribution of each anti-an-methyl-K antibody used to the definition of the K-methylome, with no single antibody outperforming the others (**B**) Intensity density distribution comparing arginine-and lysine methylated peptides to Met-0/Met-4 containing (un-methylated) peptides in the In-Gel nucleosol experiment. Un-methylated peptides from proteins with an identified methylation site have been excluded.

Figure S4. Detection of lysine-methylated sites by In-Gel and OFFGEL approaches. (A) Comparison of number of methyl-K sites obtained by the two separation approaches. **(B)** The amino acid composition of the subset of lysine-methylated peptides uniquely identified in the two techniques, excluding the methylated arginine.

Figure S5. Histones methylated peptides pairs encoded by hmSILAC-specific delta masses. A, B, C upper panels: Zoomed MS spectrum for light and heavy methyl doublets corresponding to KSAPATGGVK (27-36) peptide from Histone H3, is identified in mono-, di- and tri-methylated form, respectively. **A, B, C lower panels**: HCD MSMS spectra for the light and heavy peptides are reported. In each case the mass shifts due to the presence of the methyl group is confirmed in the characteristic b- and y- ion series. **D**, **E** upper panels: Zoomed MS spectrum for light and heavy methyl doublets corresponding to EIAQDFKTDLR (73-83) peptide from Histone H3 protein, identified in mono- and di-methylated form, respectively.. **D**, **E** lower panel: -b and -y ion series are displaced by 4 Da and 8 Da, respectively.

Figure S6. Contribution of each experimental strategy to the Total Modified Sites annotated

Table S1. List of methylated peptides and sites

The spreadsheet named “Key for Table” includes a description of each sheet (“All Sites Non Redundant”, “All Histones”, “All Non Histones”, “Ambiguous Sites”) as well as an explanation of the included columns and abbreviations.

Supplementary References

1. J. Cox, I. Matic, M. Hilger, N. Nagaraj, M. Selbach, J. V. Olsen and M. Mann, *Nat Protoc*, 2009, **4**, 698-705.

Electronic Supplementary Material (ESI) for Molecular BioSystems

Bremang M. *et al.*, 2013 Figure S1

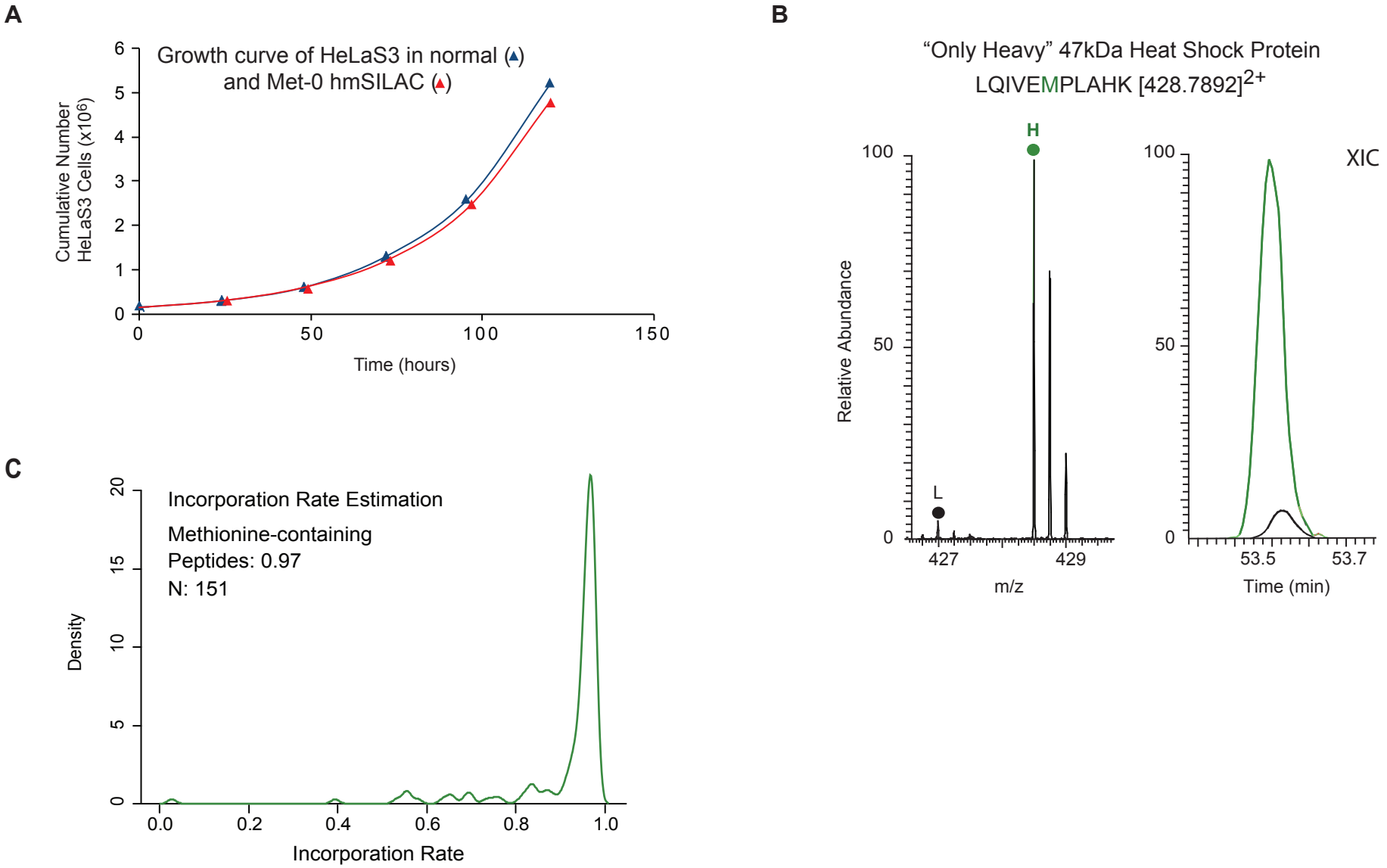

Bremang M. *et al.*, 2013 Figure S2

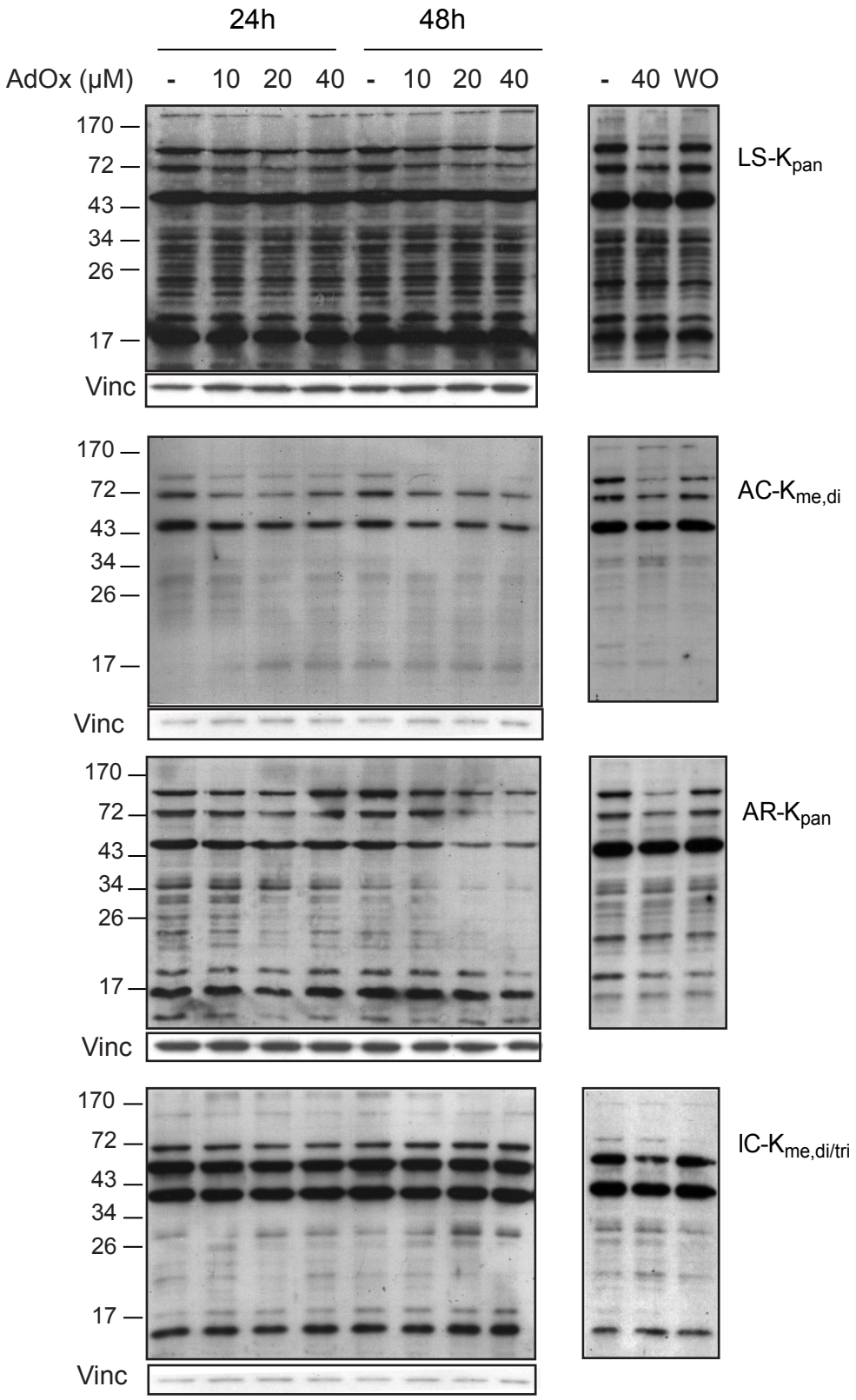

Electronic Supplementary Material (ESI) for Molecular BioSystems

Bremang M. *et al.*, 2013 Figure S3

A

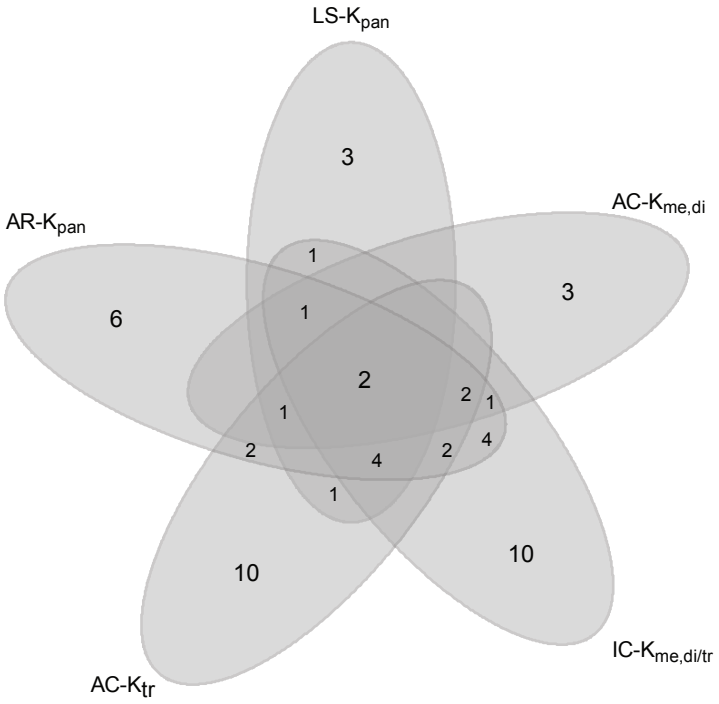

B

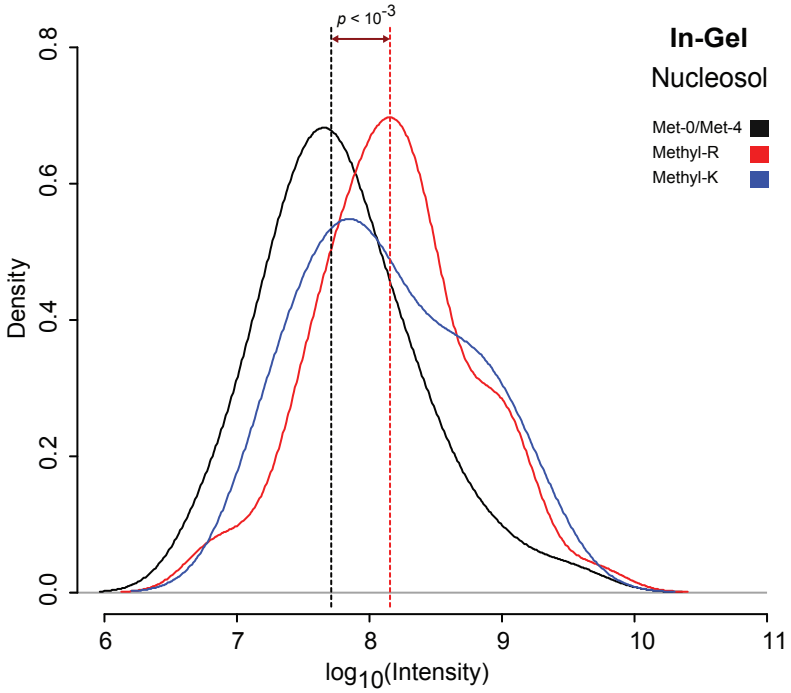

Bremang M. *et al.*, 2013 Figure S4

A

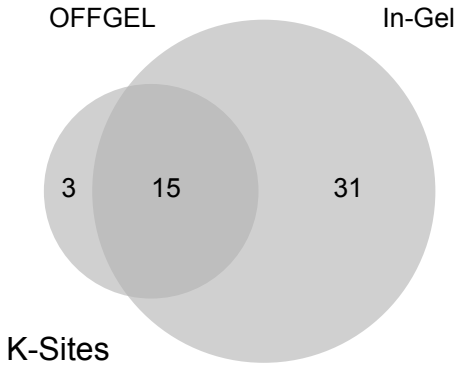

B

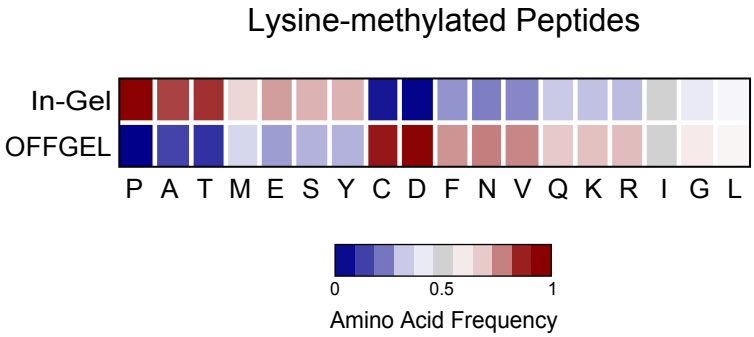

H3F3A
K(me1)SAPATGGVK (27-36)

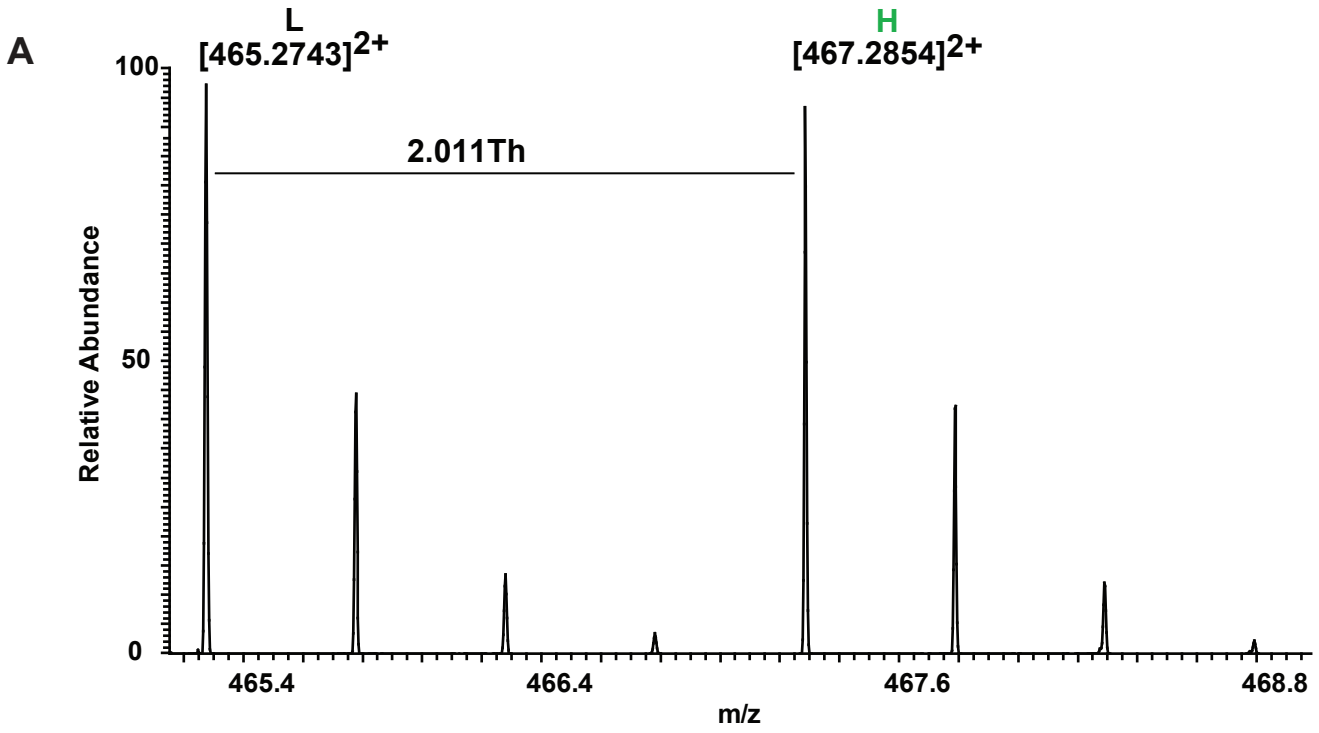

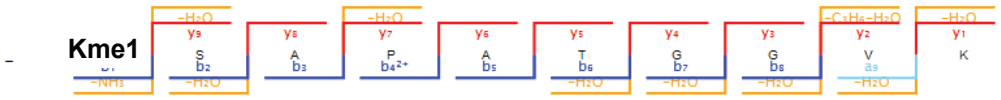

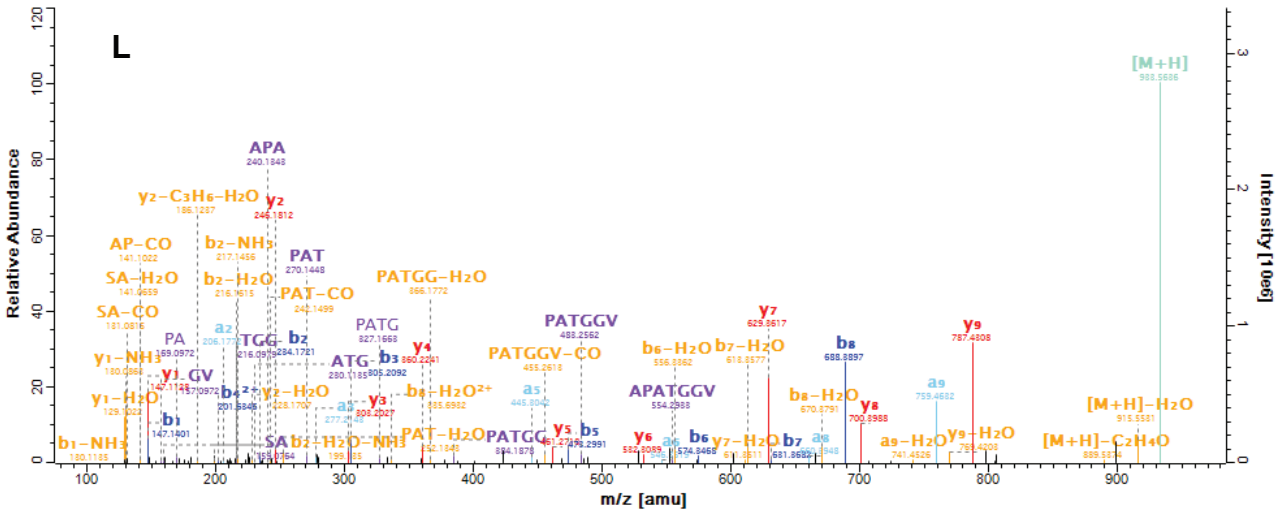

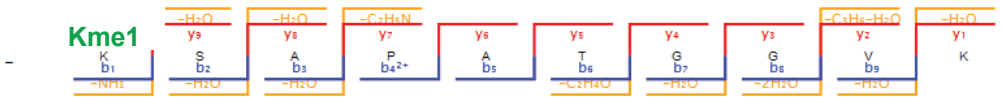

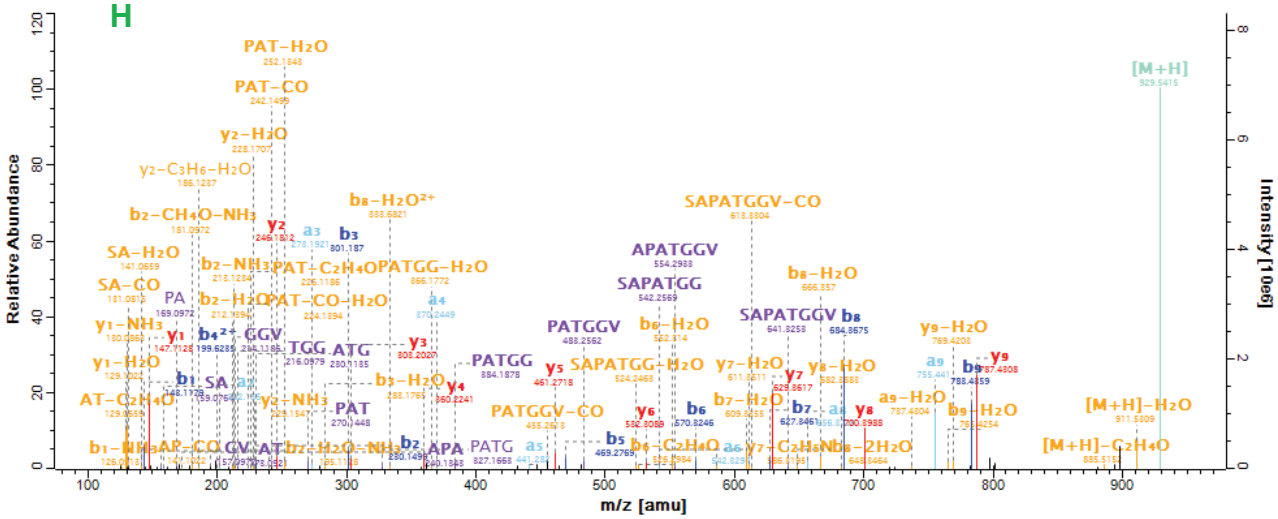

H3F3A
K(me2)SAPATGGVK (27-36)

B

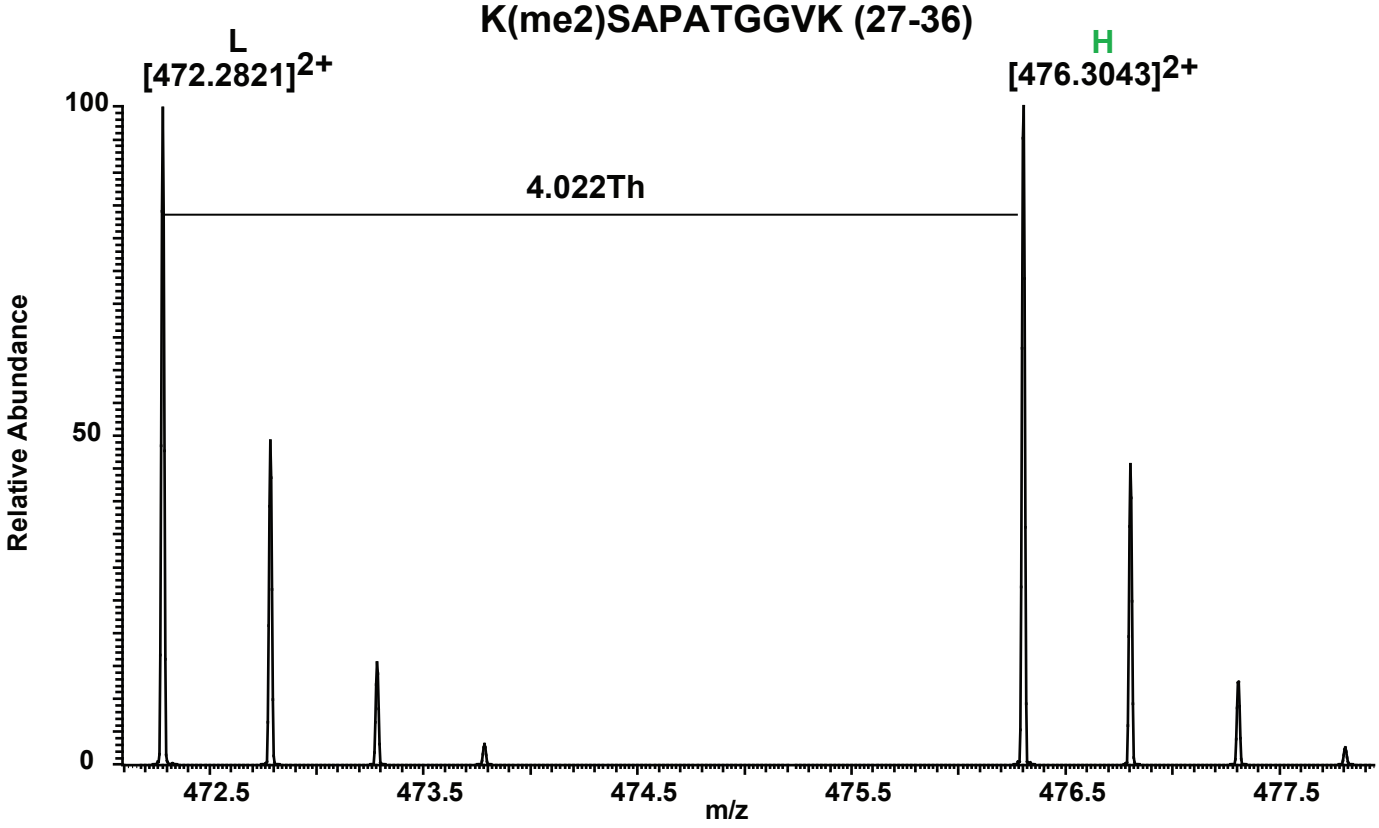

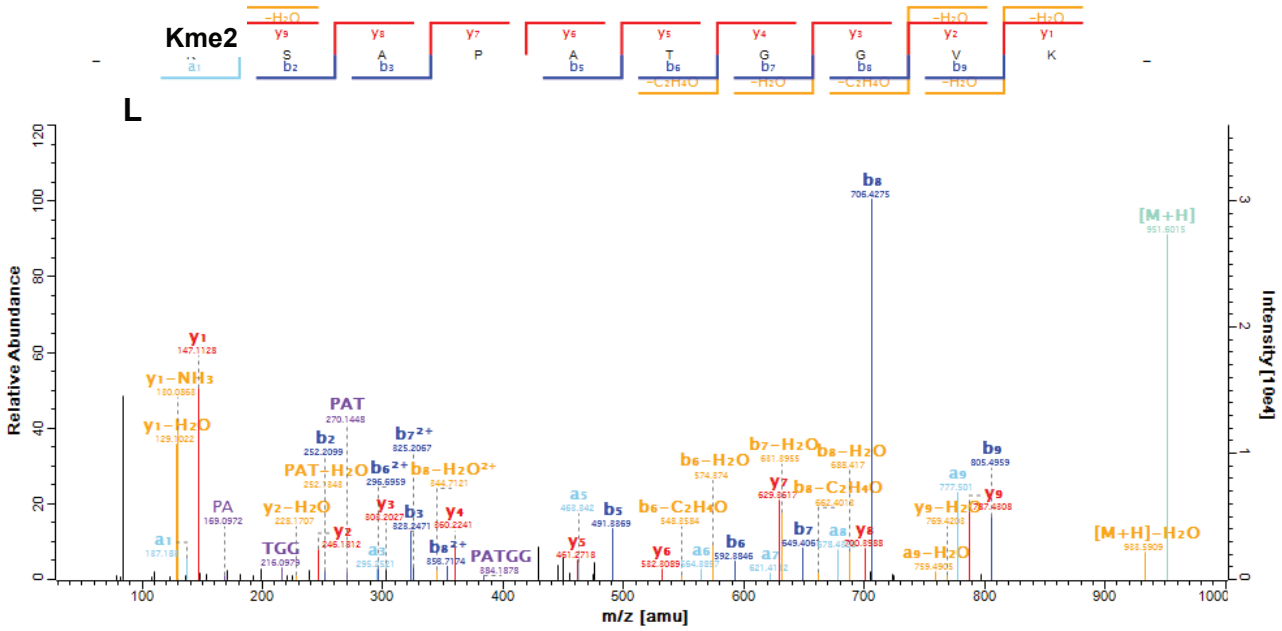

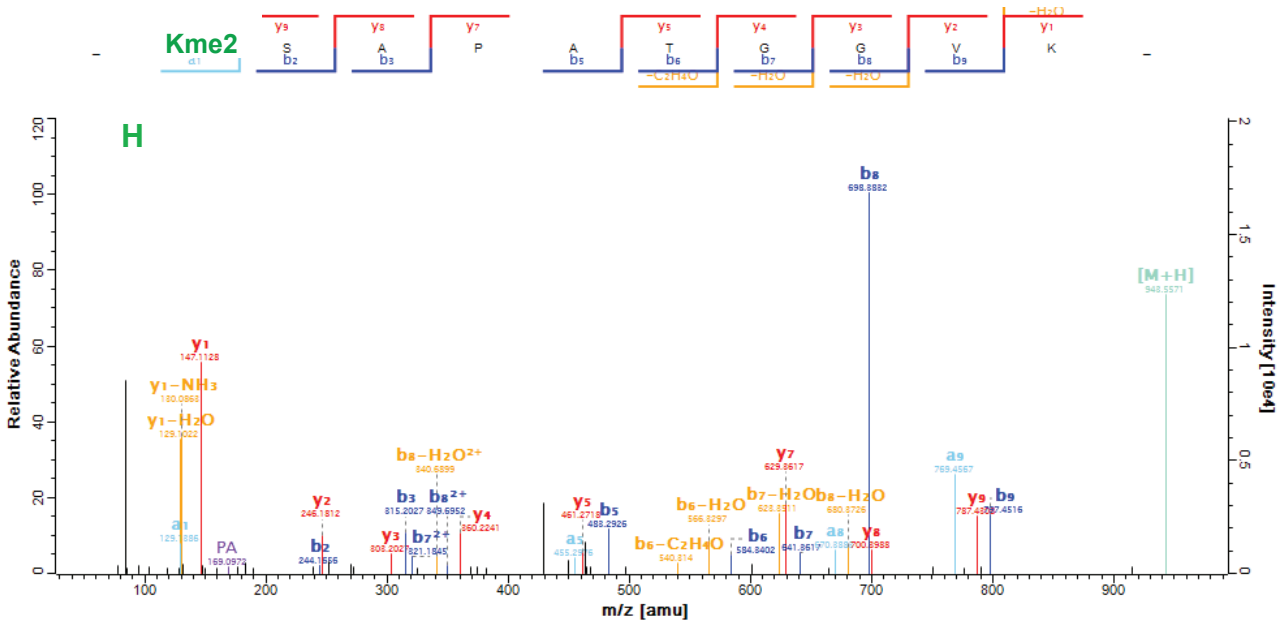

H3F3A
K(me3)SAPATGGVK (27-36)

C

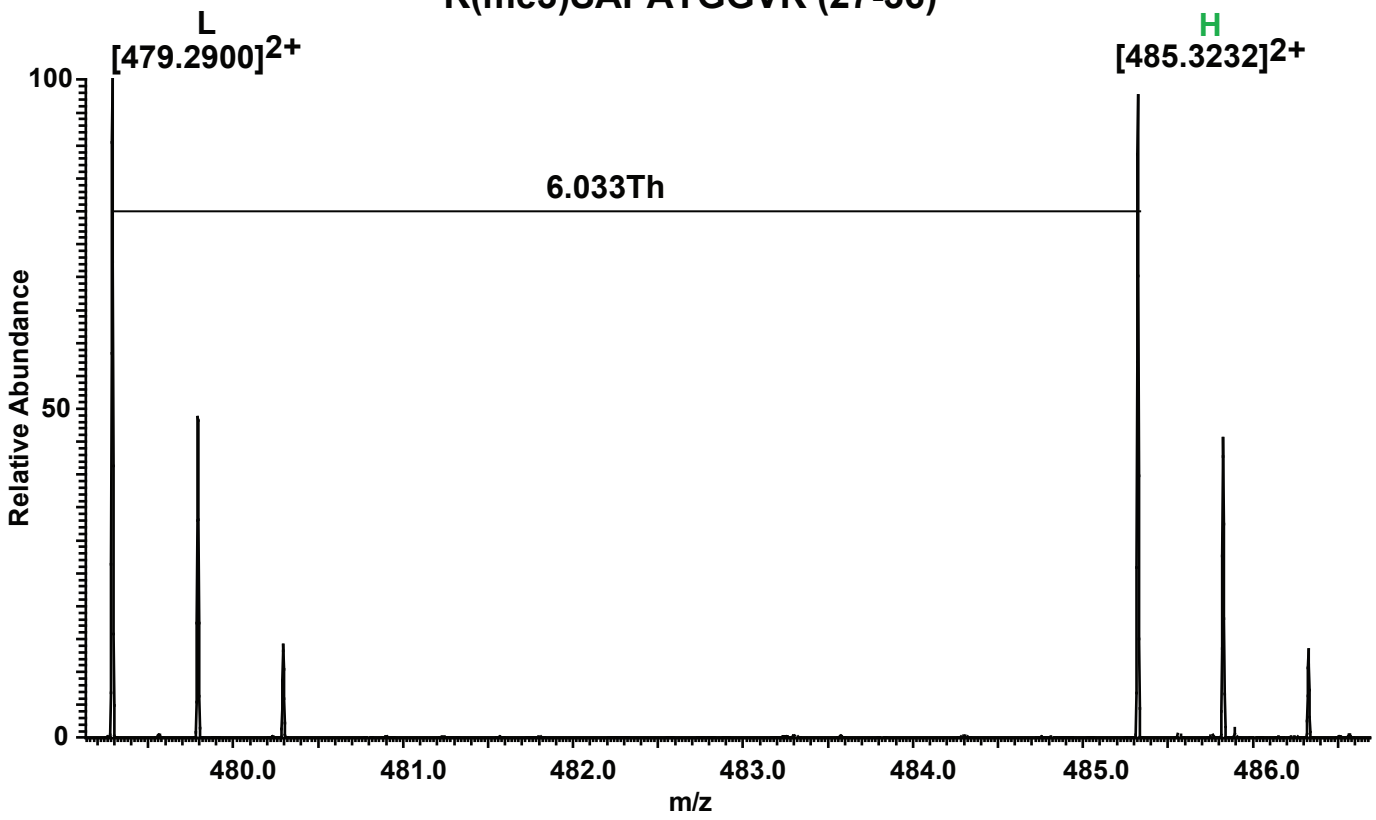

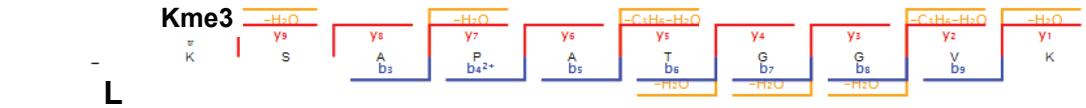

L

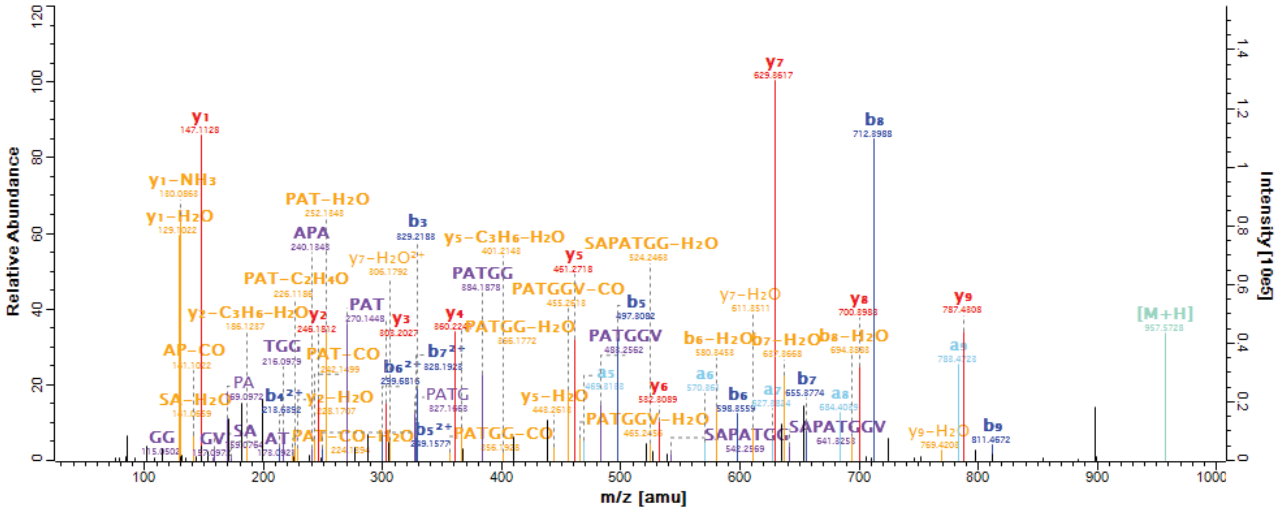

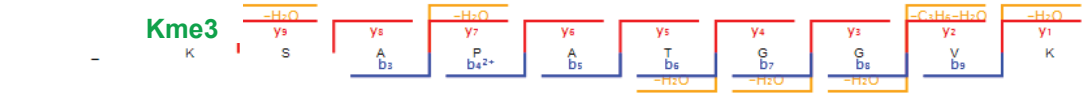

H

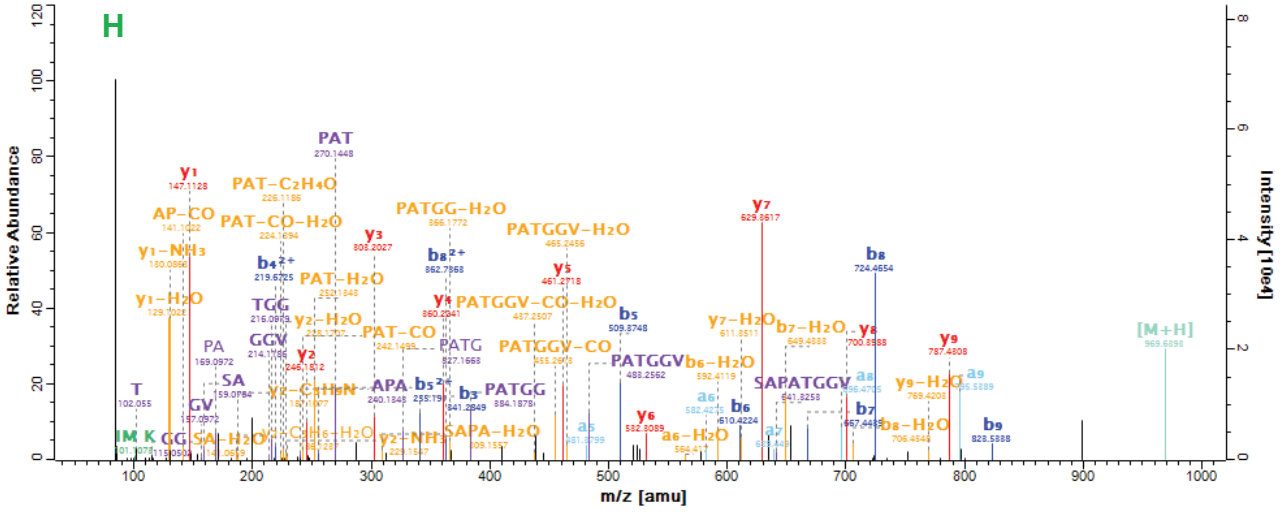

H3F3A

Bremang M. *et al.*, 2013 Figure S5

EIAQDFK(me1)TDLR (73-83)

D

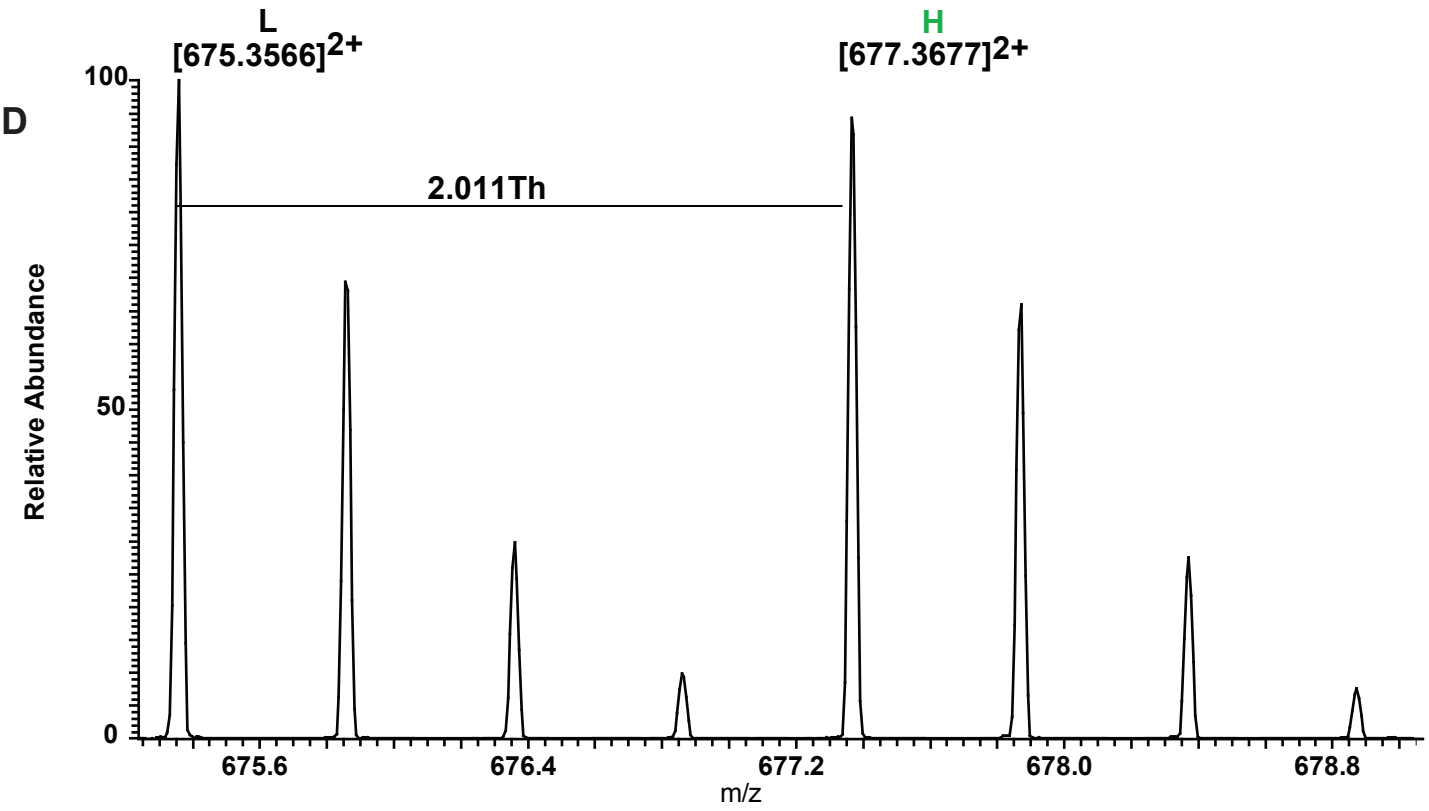

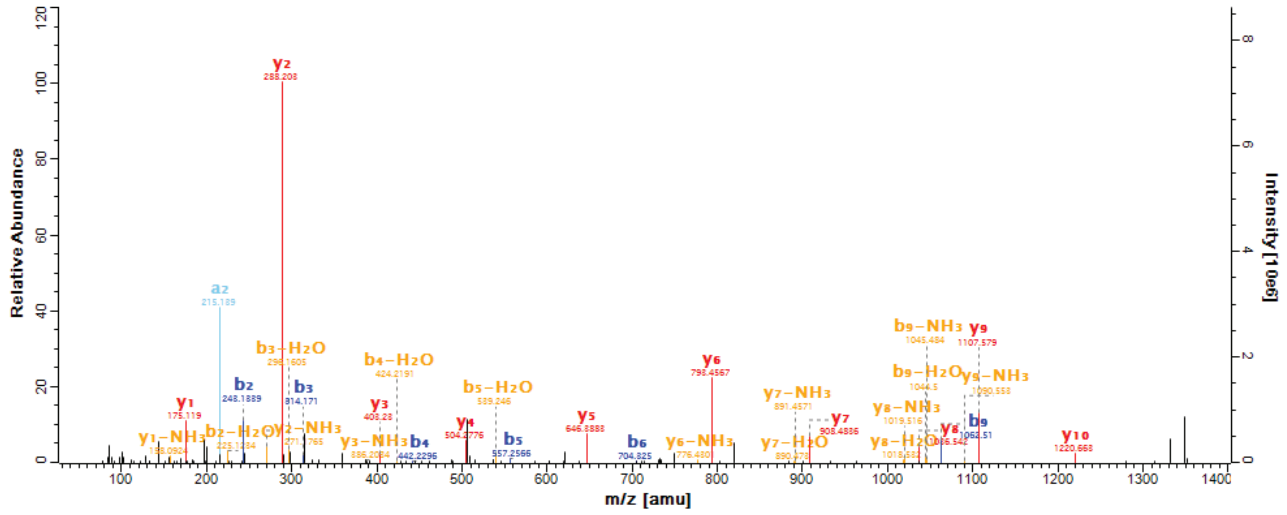

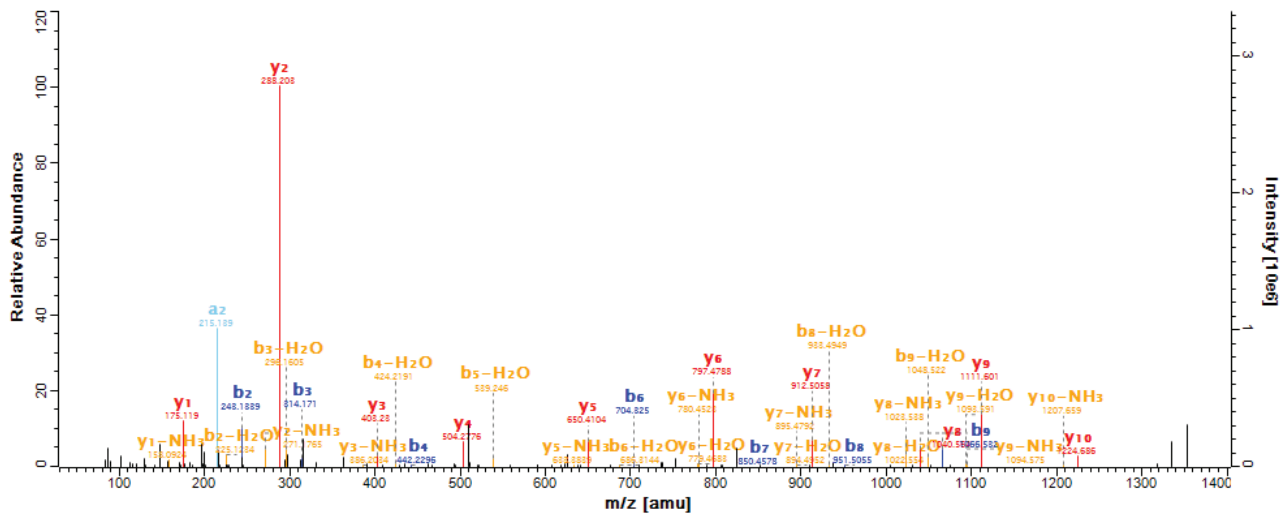

H3F3A

EIAQDFK(me2)TDLR (73-83)

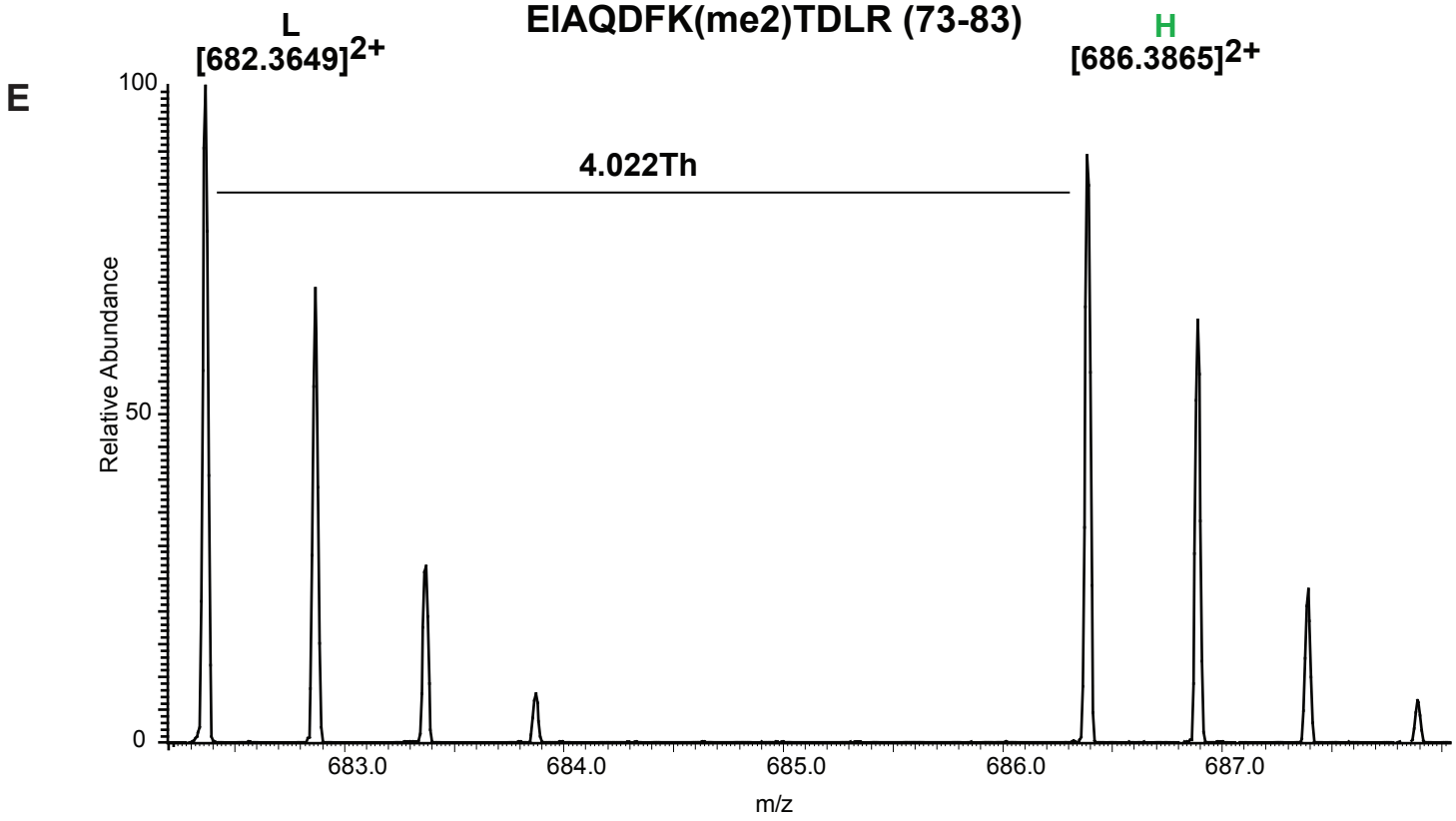

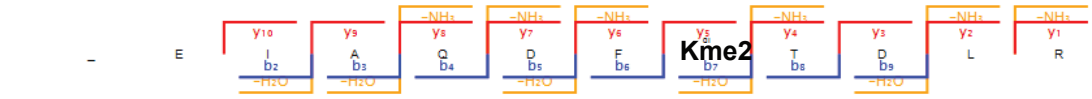

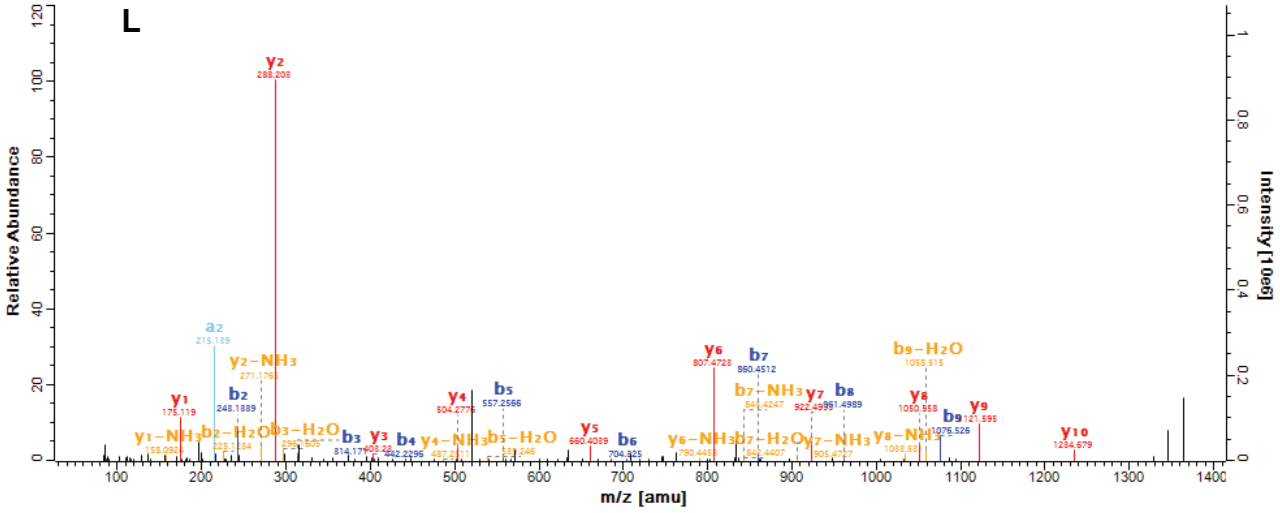

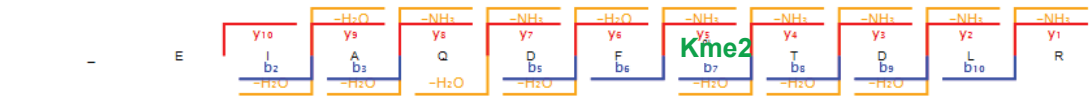

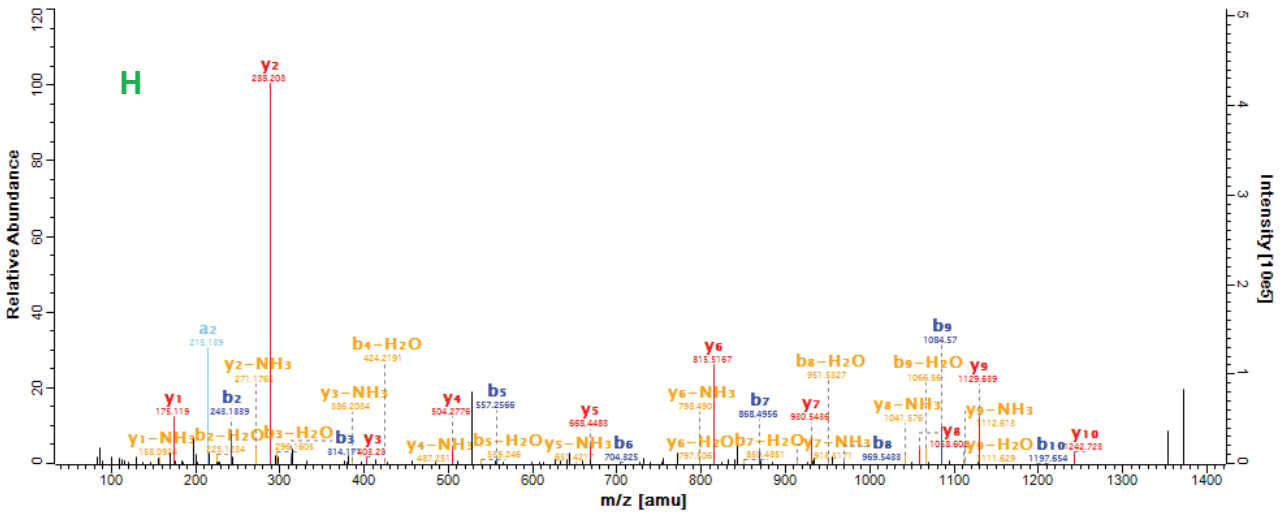

Bremang M. *et al.*, 2013 Figure S6

A Methyl-K Sites

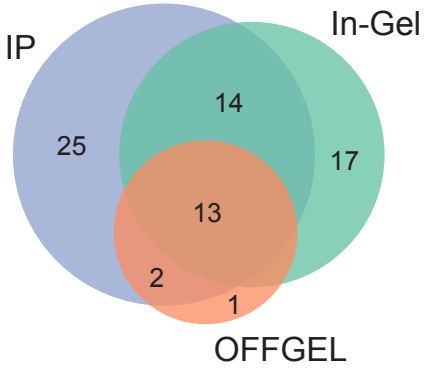

B Methyl-R Sites